PHASE, a Universal Software Package for the Propagation of Time-Dependent Coherent Light Pulses along Grazing Incidence Optics

J. Bahrdt*[a], U. Flechsig[b], S. Gerhardt[c], I. Schneider[d]
[a]Argonne National Laboratory, 9700 S. Cass Avenue, Argonne, Il 60439, USA
[b]Paul-Scherrer-Institut, 5232 Villigen PSI, Switzerland
[c]Humboldt-Universität Berlin, Unter den Linden 6, 10117 Berlin, Germany
[d]Freie Universität Berlin, Arnim Allee 14, 14195 Berlin, Germany

ABSTRACT

The software package PHASE includes routines for the propagation of coherent light within the stationary phase approximation (SPA). The code is based on a nonlinear analytic transformation of electric field arrays across longitudinally extended optical elements in normal and grazing-incidence geometries. Recently, the representation of the optical elements (OEs) has been extended to 8th-order polynomials in the OE-coordinates. Strongly curved mirror surfaces can be treated and systematic fabrication errors can be modeled up to 8th order. Each element is represented by an individual matrix and the combination of several elements is accomplished by simple matrix multiplications. The SPA-method can be interpreted as a thick lens approximation, whereas the Fourier Optics algorithm deals with thin lenses. Both methods have advantages and disadvantages. Recently, the PHASE package has been extended to Fourier Optics methods. The appropriate propagator or even a combination of different propagators can be selected from the same interface, which is running under IDL. This permits a one-by-one comparison of both methods via the same interface, which helps to evaluate the advantages and limitations of both methods.

Keywords: physical optics, propagation of coherent light

1. INTRODUCTION

In physical optics the Fourier Optics (FO) method is a widely used tool for wave propagation along optical elements. Extensive use of the fast Fourier transformation algorithm (FFT) keeps the computation time low. Most optics can be simulated in this way. There are, however, cases, where the limits of the FO method become apparent (strong demagnifications or long mirrors at grazing incidence angles) and another physical optics approach is better suited: the package PHASE has been developed over many years at BESSY / HZB. The computing algorithm is based on a repeated evaluation of integrals of the form in Eq.1 using the Stationary Phase Approximation (SPA). Equation 1 represents the wave propagation across an optical element:

$$\iint g(w,l)\cdot e^{ik\varphi(w,l)}\cdot dw\cdot dl. \qquad (1)$$

The integral has to be evaluated for various combinations of initial coordinates (y,z) and final coordinates (y',z') where the integration variables are the optical element coordinates w and l. The functions g and φ depend on the coordinates (y,z,y',z'). An explicit integration is extremely time consuming; however, the computation time can reduced by orders of magnitude using the Stationary Phase Approximation (SPA). The SPA concentrates on the analysis of the critical points of the 1st kind (w_0,l_0) at the optical element surface, which are defined by the extrema of the length of the optical path that connects the points (y,z), (w_0,l_0) and (y',z') [1]. This permits the replacement of the integral by a summation of the contributions of the critical points of the 1st kind. The code is described in detail in [2-4]. So far all equations have been derived analytically using the algebraic code REDUCE [5]. The size of the code grows exponentially with the expansion order of the optical element surface polynomials. Heretofore, this limited the procedure to a 4th-order expansion in the coordinates and angles. In section 2 a new method for the code generation is presented that does not have these limitations. It is used for an extension of the code up to 7th order in the coordinates and angles (8th order in the OE surface polynomials). The gain in accuracy is illustrated for a strongly demagnifying plane ellipse. Fabrication errors as simulated with 8th-order polynomials can be analyzed as well by adding them to a perfect surface before propagation.

* on leave from Helmholtz-Zentrum Berlin, Berlin, Germany, johannes.bahrdt@helmholtz-berlin.de

Figure 1 shows the typical residual height profile of two parabolic mirrors as measured by a slope measuring profiler (NOM) [6] at HZB [7]. These two examples show the current limits of fabrication technology. The high spatial frequency is due to the size of the polishing tool applied for deterministic surface finishing (computer aided polishing (CAP), in this case). The low frequency slope errors are typical residuals of mirrors of this size, and they may produce speckle pattern for coherent illumination. The low spatial frequency part is fitted with an 8th-order polynomial, which is sufficient in this case. They can be included in the extended propagation scheme as described in this article, whereas the high frequency part has to be neglected. For large sagittal radii (>100m) another surface finishing technology, ion beam polishing, can be applied. Here, the high frequency pattern is strongly reduced, whereas the low frequency structures remain. If necessary, the high frequency part can be implemented into PHASE by a replacement of one transformation for the complete mirror by a bunch of transformations that are related to small patches of the surface where the surface function is expanded locally at the center of each patch. During propagation the individual transformation is chosen depending on where the critical point is located. The computation increases only minimally; however, the data handling needs sophisticated bookkeeping.

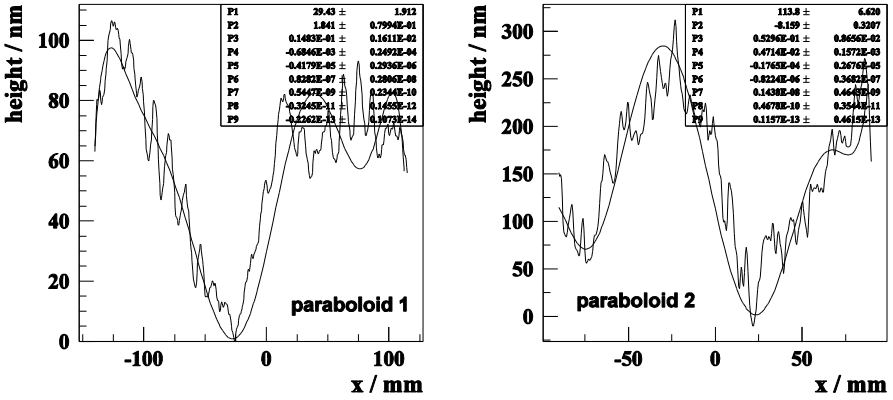

Figure 1: Profiles of residual height of two rotational symmetric parabolic mirrors as measured with the the Nanometer Optical Component Measuring Machine (NOM) at HZB [6-7]. The ideal surface profile has been subtracted. The sagittal curvature of the mirror on the right is steeper and, thus, is limiting the achievable figure accuracy by use of CAP and, as a consequence, the overall errors are larger.

Only recently, more advanced OE surface shapes, so-called diaboloids, have been discussed [8-9]. Usually, the optical elements of synchrotron radiation beamlines can be described by second-order surfaces of the form

$$F(x,y,z) = 0 = \sum_{i,j,k=0}^{2} a_{i,j,k} x^i y^j z^k .$$

For example, ellipsoids, hyperboloids, paraboloids, cylindrical surfaces and conical surfaces belong to this class of elements. A torus cannot be described in this form, since the surface is given as a 4th-order function *F(x,y,z)* where only even terms appear. It is worth noting that the representation of 2nd-order surfaces in this form is different from the PHASE parametrization that follows from solving the equation *F(x,y,z)=0* for *y*.

There are cases where other forms can improve the performance significantly. Zeschke [8] discusses a strongly demagnifying refocusing optic under astigmatic conditions. Principally, a torus mirror can handle the astigmatism; however, the optical aberrations are large. A Kirkpatrick-Baez arrangement with two plane elliptical mirrors minimizes the aberrations; however, it reduces the transmission of the beamline. Zeschke adds 3rd-order terms to the surface equation *F(x,y,z)*, which significantly improves the focus quality. Using modern fabrication technologies and a cutting-edge metrology for quality control, the production of such a mirror seems to be feasible. To design such a mirror a substrate with adaptive elements like piezoelectric electrodes, as done for Bimorph-mirrors [10], may enable a compensation of higher-order figure errors. Optimized surface geometries can be designed with successive ray tracing simulations and a scanning of the parameter space [8]. An efficient algorithm is implemented in PHASE [11]. A merit function built from specific matrix elements representing optical aberrations to be eliminated or, alternatively, from a weighted sum of the focus momenta is minimized with an efficient nonlinear minimization scheme. Expansion coefficients of the optical surfaces are used as optimization parameters. The design process will benefit from the extension of the expansion order as described in this article.

Fourier Optics propagators have been included into the PHASE package. These routines as well as the SPA algorithm can be invoked from a user friendly IDL-based interface. Depending on the requirements, either of the codes or a combination of them can be used. The availability of several propagation methods within the same program permits a direct comparison of both methods. This will be the subject of further studies.

2. EXTENSION OF THE PHASE CODE TO 8TH ORDER IN THE OPTICAL ELEMENT SURFACE COORDINATES

A new strategy for the code development

In geometrical optics (ray tracing) the light is modeled with rays that propagate through a set of optical elements (i.e., a beamline) on well-defined trajectories. The SPA method needs these rays, called principle rays, as well, since they define the critical points of the 1st kind. Within the SPA certain phase-space regions around the principle rays are integrated analytically assuming infinitely wide OE surfaces. If this approximation is not fulfilled, the diffraction effects at the OE boundary can be included via critical points of the 2nd kind on the boundary [1]. This is not yet included in PHASE because, usually, FEL beams are highly collimated, and the OEs do not scrape the beam. The SPA, which is the first term of an asymptotic expansion, assumes a quadratic behavior of the optical path around the critical points of the 1st kind. The validity of this assumption depends on the wavelength. If it is not fulfilled, the asymptotic expansion has to be extended to higher orders.

In the following we concentrate on the derivation of the formulas for the principle ray transformation from a source plane to an image plane because this part was limiting the method so far. Other parts such as the scaling factors, which account for the piecewise analytic integration or the generation of the transformation matrices, are not discussed here because they are evaluated as before [1-3]. In a first step the transformation of initial coordinates and angles (y,z,dy,dz) to final coordinates and angles *(y',z',dy',dz')* (figure 2) is derived by means of a power series expansion with respect to the initial coordinates, where the expansion ord is *ord:*

$$\begin{pmatrix} y' \\ z' \\ dy' \\ dz' \end{pmatrix} = \sum_{\substack{i,j,k,l \\ 0 \le i+j+k+l \le ord}} \begin{pmatrix} ypc(i,j,k,l) \\ zpc(i,j,k,l) \\ dypc(i,j,k,l) \\ dzpc(i,j,k,l) \end{pmatrix} \cdot y^i z^j dy^k dz^l. \qquad (2)$$

Based on this transformation, for each optical element a matrix is derived that describes the nonlinear transformation across this optical element. A multiplication of the matrices yields the nonlinear transformation for a set of elements. The procedure used heretofore makes extensive use of the algebraic code REDUCE to derive the expansion coefficients *ypc*, *zpc*, *dypc*, *dzpc*. This "brute force" method is not applicable for expansion orders above 4. A new strategy, which has successfully been applied to a 7th order expansion, will be described below. The principle rays are defined by the extrema of the optical path length, i.e., their zero 1st derivatives with respect to the OE coordinates. The optical path length across an element (mirror or grating) is expressed in the form of Eq. 3.

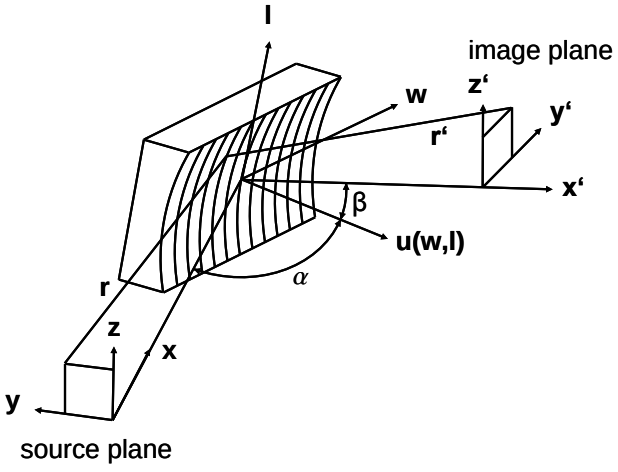

Figure 2. Definition of coordinate systems.

$$F = \sqrt{(\tilde{x}-u)^2+(\tilde{y}-w)^2+(\tilde{z}-l)^2}+\sqrt{(\tilde{x}'-u)^2+(\tilde{y}'-w)^2+(\tilde{z}'-l)^2}+\frac{wm\lambda}{d}, \quad (3)$$

$$\tilde{x} = r\cdot cos(\alpha)+y\cdot sin(\alpha),$$

$$\tilde{y} = r\cdot sin(\alpha)-y\cdot cos(\alpha),$$

$$\tilde{z} = z,$$

$$\tilde{x}' = r'\cdot cos(\alpha)-y'\cdot sin(\alpha),$$

$$\tilde{y}' = r'\cdot sin(\alpha)+y'\cdot cos(\alpha),$$

$$\tilde{z}' = z'.$$

The optical element coordinates *u*, *w* and *l* are defined in figure 2 where *u* describes the optical element surface being the height deviation with respect to a plane mirror. *u* is expanded in a power series with respect to *w* and *l*.

The partial derivatives of the optical path function *F* with respect to *w* and *l* are

$$\partial F/\partial w = 0 \text{ and} \quad (4)$$

$$\partial F/\partial l = 0. \quad (5)$$

They reveal the correlation of initial and final coordinates in an implicit manner. Equations 4-5 are expanded in a Taylor series with respect to the variables *w, l, y, z, y', z'* where we call the expansion coefficients m_1 and m_2. In a first step Eq. 4-5 are solved for *y'* and *z'*. The final coordinates *y'* and *z'* depend on *w, l, y, z*, and we represent them as a power series expansion in *w, l, y, z* with the coefficients $ypc_1(i,j,k,l)$ and $zpc_1(i,j,k,l)$, where *i, j, k, l* are the exponents of the variables *w, l, y, z*. Inserting this Taylor series into Eq. 4-5 we end up with two equations dependent on the variables *w, l, y, z*, which are used for the evaluation of the coefficients $ypc_1(i,j,k,l)$ and $zpc_1(i,j,k,l)$. Both equations have terms proportional to $w^i l^j y^k z^l$. Since these variables are independent from each other, the prefactors of all cross products have to be equal to zero. This permits an iterative solution of a set of equations which is described in [2-3]. In the past the algebraic code REDUCE [5] has been used for the iterative solution of pairs of coupled linear equations yielding the expansion coefficients $ypc_1(i,j,k,l)$ and $zpc_1(i,j,k,l)$. The source code as produced by REDUCE increases exponentially with the order *ord+1* of the surface polynomial *u(w,l)*, and so far the code is limited to a 5th-order surface polynomial because higher orders could be handled neither with REDUCE nor with a FORTRAN compiler. Therefore, extending the transformations to higher orders requires another strategy that will be described in the following. Similar to the approach in [2-3] the coupled linear equations are solved iteratively, going from the lowest-order terms to higher orders and making use of the results already obtained. For each pair of coefficients $ypc_1(i,j,k,l)$ and $zpc_1(i,j,k,l)$ a pair of coupled linear equations has to be solved:

$$a_1\cdot ypc_1(i,k,s,t)+b_1\cdot zpc_1(i,k,s,t)+c_1(i,k,s,t)=0 \text{ and} \quad (6)$$

$$a_2\cdot ypc_1(i,k,s,t)+b_2\cdot zpc_1(i,k,s,t)+c_2(i,k,s,t)=0. \quad (7)$$

The lowest order terms of Eq. 4-5, $ypc_1(0,0,0,0)$ and $zpc_1(0,0,0,0)$, are evaluated with a two-dimensional Newton Raphson method. Then, the coefficients $a_{1/2}$ and $b_{1/2}$, which are independent of *i, k, s, t*, are determined from:

$$a_{1/2} = \sum_{0\le n5+n6\le ord} m_{1/2}(0,0,0,0,n5,n6)\cdot ypc_1(0,0,0,0)^{n5-1}n5\cdot zpc_1(0,0,0,0)^{n6} \text{ and} \quad (8)$$

$$b_{1/2} = \sum_{0\le n5+n6\le ord} m_{1/2}(0,0,0,0,n5,n6)\cdot ypc_1(0,0,0,0)^{n5}\cdot zpc_1(0,0,0,0)^{n6-1}n6. \quad (9)$$

For each quadruple *i, k, s, t*, which is related to the coefficients $ypc_1(i,k,s,t)$ and $zpc_1(i,k,s,t)$, the constants c_1 and c_2 are evaluated from:

$$c_{1/2} = \sum_{j=0}^{i}\sum_{m=0}^{k}\sum_{u=0}^{s}\sum_{v=0}^{t} \sum_{\substack{0\le n5+n6\le \\ ord-j-m-u-v}} m_{1/2}(j,m,u,v,n5,n6) \tag{10}$$

$$\cdot\left\{\sum_{\substack{condition \\ Eq.11}} \prod_{p=1}^{n5} ypc_1(d_{p1},d_{p2},d_{p3},d_{p4}) \prod_{p=1}^{n6} zpc_1(e_{p1},e_{p2},e_{p3},e_{p4})\right\}.$$

The expressions $m_{1/2}(j,m,u,v,n5,n6)$ are the expansion coefficients of Eq. 4-5 with respect to w ,l ,y ,z ,y' ,z'. The products in the bracket are equal to 1 for $n5$=0 or $n6$=0, respectively. The sum in the bracket runs over all product combinations that fulfill the conditions as defined in Eq. 11:

$$\sum_{p1=1}^{n5} d_{p1} + \sum_{p1=1}^{n6} e_{p1} = i-j \quad \wedge \quad \sum_{p2=1}^{n5} d_{p2} + \sum_{p2=1}^{n6} e_{p2} = k-m \quad \wedge \tag{11}$$

$$\sum_{p3=1}^{n5} d_{p3} + \sum_{p3=1}^{n6} e_{p3} = s-u \quad \wedge \quad \sum_{p4=1}^{n5} d_{p4} + \sum_{p4=1}^{n6} e_{p4} = t-v \quad \wedge$$

$$d_{px} \le i,k,s,t \ \wedge \ e_{px} \le i,k,s,t \ \forall x \in \{1,2,3,4\} \ \wedge \ (d_{p1},d_{p2},d_{p3},d_{p4}) \ne (i,k,s,t) \ \wedge \ (d_{p1},d_{p2},d_{p3},d_{p4}) \ne (i,k,s,t).$$

As a result, we get the expansions:

$$y' = \sum_{i,j,k,l} ypc_1(i,j,k,l) w^i l^j y^k z^l \quad \text{and} \quad z' = \sum_{i,j,k,l} zpc_1(i,j,k,l) w^i l^j y^k z^l. \tag{12}$$

In the next step we evaluate the expansion coefficients of w and l with respect to y, z, dy, dz. The initial angles are related to the mirror coordinates and the initial coordinates via

$$dy = \frac{u\cdot\sin(\alpha) - w\cdot\cos(\alpha) - y}{r - u\cdot\cos(\alpha) - w\cdot\sin(\alpha)} \quad \text{and} \quad dz = \frac{l-z}{r - w\cdot\sin(\alpha) - u\cdot\cos(\alpha)}. \tag{13}$$

Inserting a power series representation of w and l into these equations provides two power series expansions in the variables y, z, dy, dz. Each individual term must be zero, which gives a set of equations defining the expansion coefficients $wc(y,z,dy,dz)$ and $lc(y,z,dy,dz)$ of w and l. Again these equations can be solved iteratively, starting with the lowest-order terms. The iterative procedure follows exactly the same as the evaluation of the coefficients ypc_1 and zpc_1 with one exception: The term $lc(0,0,0,0)$ is assumed to be zero, which means that $wc(0,0,0,0)$ can be determined with a one-dimensional instead of a two-dimensional Newton Raphson routine.

Now, the power series expansions of w and l are inserted into Eq. 12, yielding the coordinates y' and z' as Taylor series expansions in the variables y, z, dy, dz. The expansion coefficients are derived from

$$\begin{pmatrix} ypc(i,k,s,t) \\ zpc(i,k,s,t) \end{pmatrix} = \sum_{j=0}^{i}\sum_{m=0}^{k} \sum_{n5+n6=0}^{ord-j-m} \begin{pmatrix} ypc_1(n5,n6,j,m) \\ zpc_1(n5,n6,j,m) \end{pmatrix} \tag{14}$$

$$\cdot\left\{\sum_{\substack{condition \\ Eq.15}} \prod_{p=1}^{n5} wc(d_{p1},d_{p2},d_{p3},d_{p4}) \prod_{p=1}^{n6} lc(e_{p1},e_{p2},e_{p3},e_{p4})\right\}$$

with conditions as defined in Eq.15:

$$\sum_{p1=1}^{n5} d_{p1} + \sum_{p1=1}^{n6} e_{p1} = i - j \quad \wedge \quad \sum_{p2=1}^{n5} d_{p2} + \sum_{p2=1}^{n6} e_{p2} = k - m \quad \wedge \tag{15}$$

$$\sum_{p3=1}^{n5} d_{p3} + \sum_{p3=1}^{n6} e_{p3} = s \quad \wedge \quad \sum_{p4=1}^{n5} d_{p4} + \sum_{p4=1}^{n6} e_{p4} = t \quad \wedge$$

$d_{px} \le i,k,s,t \ \wedge \ e_{px} \le i,k,s,t \ \forall x \in \{1,2,3,4\}$.

Finally, *dy'* and *dz'* given as

$$dy' = \frac{u \cdot \sin(\beta) - w \cdot \cos(\beta) + y'}{r' - u \cdot \cos(\beta) - w \cdot \sin(\beta)} \quad \text{and} \quad dz' = \frac{l - z'}{r' - w \cdot \sin(\beta) - u \cdot \cos(\beta)} \tag{16}$$

have to be expressed in a power series of *y*, *z*, *dy*, *dz*. The power series expansions of *w*, *l*, *y' ,z'* are already known. The power series of *u(w,l)*,

$$u(w,l) = \sum_{n1+n2=0}^{ord} uc(n1,n2)\, w^{n1} l^{n2}, \tag{17}$$

has to be converted into a Taylor series with variables *y*, *z*, *dy*, *dz*. At this point we may skip the expansion terms of *u* of order *ord+1*, whereas in Eq. 3-5 they are needed due to the partial derivatives. The coefficients $uc_1(i,k,s,t)$ are derived by solving the following set of equations:

$$uc_1(i,k,s,t) = \sum_{n1+n2=0}^{ord} uc(n1,n2) \tag{18}$$

$$\cdot \left\{ \sum_{\substack{condition \\ Eq.19}} \prod_{p=1}^{n5} wc(d_{p1},d_{p2},d_{p3},d_{p4}) \prod_{p=1}^{n6} lc(e_{p1},e_{p2},e_{p3},e_{p4}) \right\}$$

with conditions as defined in Eq. 19:

$$\sum_{p1=1}^{n5} d_{p1} + \sum_{p1=1}^{n6} e_{p1} = i \quad \wedge \quad \sum_{p2=1}^{n5} d_{p2} + \sum_{p2=1}^{n6} e_{p2} = k \quad \wedge \tag{19}$$

$$\sum_{p3=1}^{n5} d_{p3} + \sum_{p3=1}^{n6} e_{p3} = s \quad \wedge \quad \sum_{p4=1}^{n5} d_{p4} + \sum_{p4=1}^{n6} e_{p4} = t \quad \wedge$$

$d_{px} \le i,k,s,t \ \wedge \ e_{px} \le i,k,s,t \ \forall x \in \{1,2,3,4\}$.

Inserting all expansions into Eq. 16 and dividing the power series of nominators and denominators gives the expansions of *dy'* and *dz'*. Thus, we have the expansion coefficient for the transformation in Eq. 2 and transformation matrices can be evaluated from the results as described in [2-3]. The size of the matrix depends on the expansion order as summarized in Table 1. The computing time for the map generation increases by more than one order of magnitude per expansion order, but it is still in the range of minutes for the 7th order. The map has to be evaluated only once for a certain geometry.

The equations above have been programmed in FORTRAN and they have substituted the original REDUCE code. With the new compact description, the size of the code shrunk by a factor of fifty. Principally, the code is not limited to 8th order, though the computation time on a single processor computer defines a limit. If the code will be transferred to a multi-core machine, higher expansion orders are reasonable.

Table 1: The size of the transformation matrix, the computation time for the matrix generation, and the ray tracing time for 1e6 rays dependent on the expansion order. The times have been measured for an Intel Q9400, 2.66-MHz, four-core processor.

Order of expansion	*Matrix Size*	*Map generation time*	*Ray tracing time*
3	*35 x 35*	*<< 1s*	*2s*
4	*70 x 70*	*<< 1s*	*4s*
5	*126 x 126*	*1s*	*7s*
6	*210 x 210*	*13s*	*10s*
7	*330 x 330*	*173s*	*16s*

Accuracy and expansion order

Depending on the optic design and accuracy requirements, the order of evaluation can be adapted appropriately. For illustration, the focusing properties of the plane ellipse as planned for the SWISS-FEL high-energy Aramis beamline at 12.4keV have been analyzed. The FEL source size and divergence are 20µm and 20µrad in both directions, respectively. The plane ellipse de-magnifies the source by a ratio of 125m : 1m at a grazing incidence angle of 2mrad. The mirror size is 500mm x 10mm, and slope errors are set to zero for clarity. The graphs of Fig. 3 have been evaluated for 7th-order expansion of the final coordinates with respect to the initial coordinates. The effect of the individual expansion coefficients *uc(i,0)* of the surface function *u(w,l)* are separated: In Figure 3, top left, all coefficients are zero apart from *uc(2,0).* The next plots show the results with more expansion coefficients *uc(i,0),* compensating the coma ($\sim dy^2$), spherical aberrations ($\sim dy^3$), higher order coma ($\sim dy^4$) and higher order spherical aberrations ($\sim dy^5$). No difference is observed between the last two graphs showing the foci for 6th-order and 8th-order surface polynomial truncation. A 5th-order expansion (6th-order surface polynomial) is sufficient in this specific case.

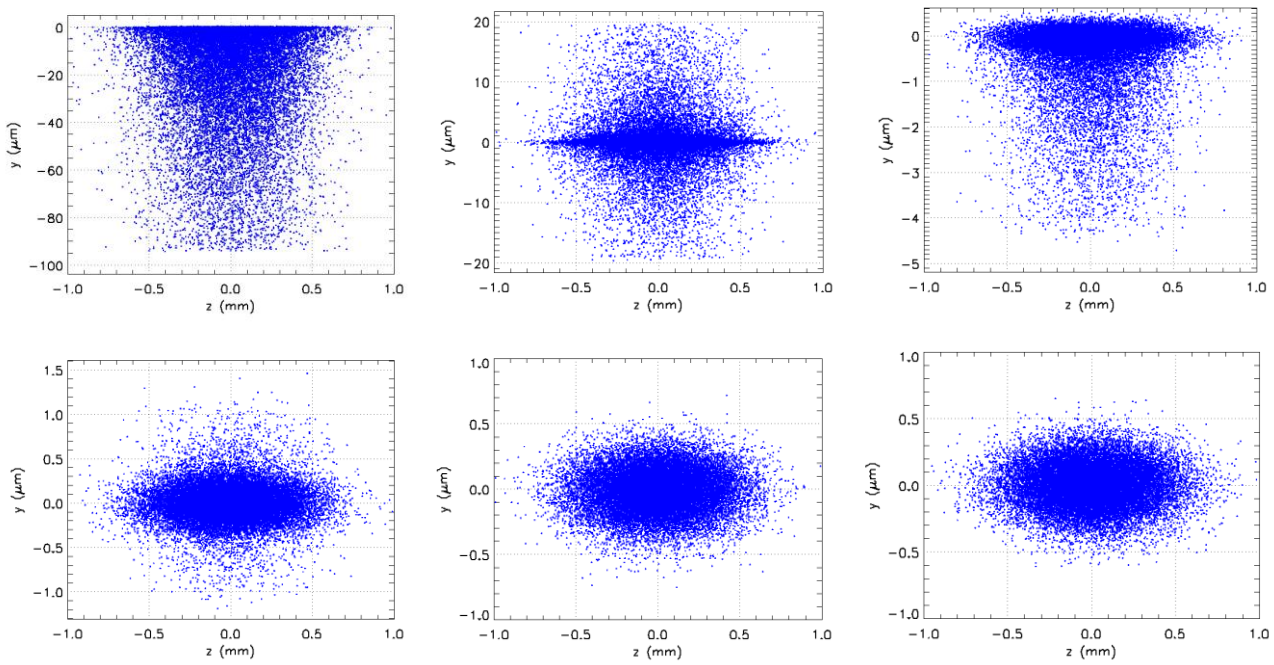

Figure 3. Focusing properties of a plane ellipse as planned for the SWISS-FEL-12keV beamline. The simulations have been performed to 7th-order expansion with respect to the initial coordinates. The mirror surface function *u(w,l)* has been truncated after 2nd, 3rd, 4th, 5th, 6th, 8th order (top left to bottom right).

3. NON-QUADRATIC PATH LENGTH TERMS

The stationary phase approximation is based on an analytic integration around the principle rays. This approach reduces the multidimensional integrations by two orders. The analytic 2-dimensional integration assumes a quadratic dependence of the optical path length on the OE coordinates *w* and *l* for fixed initial and final coordinates. The integrals can be extended to infinity if the quadratic shape is given in the range of large contributions to the integral. The double integral over *w* and *l* is proportional to

$$\left|\frac{\partial^2 PL}{\partial \Delta w^2}\cdot\frac{\partial^2 PL}{\partial \Delta l^2}-\left(\frac{\partial^2 PL}{\partial \Delta w\cdot\partial \Delta w}\right)^2\right|^{-1/2}. \tag{20}$$

The variables Δw and Δl are the distances to the critical point (w_0, l_0). Obviously, the expression diverges in case of focal conditions in one or the other plane where the 2nd derivatives with respect to Δw or Δl vanish. But even if the 2nd derivatives are non-zero, the quadratic behavior of the path length is not given if two principle rays are closely located to each other [4]. In these cases Eq. 20 is wrong. Usually these cases can be avoided by changing the geometry (shifting the source plane). Alternatively, a 3rd-order term can be added to the path length and an analytic integration is still possible. This enhances the robustness of the algorithm. The path length is rewritten as

$$PL = a\cdot w^2 + 2b\cdot w\cdot l + c\cdot l^2 + d\cdot w^3 \qquad a\neq 0. \tag{21}$$

The following coordinate transformation

$$\tilde{l} = l + \frac{b}{a}w \qquad \tilde{w} = w \tag{22}$$

removes the cross term

$$PL = a\cdot\tilde{l}^2 + \left(c-\frac{b^2}{a}\right)\cdot\tilde{w}^2 + d\cdot\tilde{w}^3 = \tilde{a}\cdot\tilde{w}^3 + \tilde{b}\cdot\tilde{w}^2 + \tilde{c}\cdot\tilde{l}^2. \tag{23}$$

With this substitution the double integral over the path length can be separated, and the integration over $\tilde{w}$ and $\tilde{l}$ can be done independently. The integral over the $\tilde{w}$-dependent terms is expanded into an analytic sum of the form

$$\int_{-\infty}^{+\infty} cos\left(\tilde{a}\cdot\tilde{w}^3+\tilde{b}\cdot\tilde{w}^2\right)d\tilde{w} \approx \frac{1}{3}\left(\sum_{k=0}^{ord}\frac{\tilde{b}^k+\left(-\tilde{b}\right)^k}{k!}|\tilde{a}|^{\frac{-2k-1}{3}}\Gamma\left(\frac{2k+1}{3}\right)cos\left(\frac{1-k}{6}\pi\right)\right), \tag{24}$$

and similarly for the sin-term. The sum on the right-hand side equals the integral on the left if the summation is extended to infinity. The accuracy in dependence on the truncation order *ord* will be the subject of further investigation.

4. FURTHER DEVELOPMENTS

Integration of Fourier Optics Algorithms into PHASE

Within Fourier Optics most beamline geometries can be evaluated either with the near-field or the far-field operator. In the near-field approach the electric field distribution in the source plane is decomposed into plane waves with different directions via an FFT operation. The plane waves are propagated by multiplication with a phase factor that depends on the propagation distance. Then, a reverse FFT is applied to the result to receive the fields in real space. The far-field approach starts from a point-spread function that describes the propagation of a point source. The point-spread function is convoluted with the electric field distribution in the source plane. Both methods are mathematically equivalent; however, the appropriate propagator has to be chosen to keep the noise level low. Another issue that influences the choice is the grid size, which is constant in the near-field approach and varies in the far-field case. For long propagation distances, the so-called Fraunhofer approximation is applicable, and the electric field distribution in the image plane is proportional to the Fourier transform of the field distribution in the source plane divided by the propagation distance. FFTs are performed on plane grids. Cutting a bent wavefront may introduce many phase oscillations that do not carry additional information apart from the bending radii. O. Chubar presented an algorithm for the removal of the oscillations before propagation and addition of the curvature later on to the result [12].

The three Fourier Optics propagators as well as the phase removal scheme have been implemented into the PHASE package. For cross checks, the integration of the Fresnel-Kirchhoff integral is included as well. Though it is extremely

slow, it is transparent and well suited for test purposes. A bunch of functions for the source generation and data preparation are also available (Table 2).

Table 2. Routines available under IDL.

source generation	*Gaussian beam / beam from file* *alternatively electric fields or amplitudes and phase*
grid manipulation	*interpolation, cuts*
propagation	*near field / far field / Fraunhofer case* *explicit integration of Fresnel Kirchhoff integral* *efficient handling of fast oscillations*
graphic output	*IDL routines*
data compression	*HDF5, variable compression rate*
interfacing to other codes	*HDF5*
interfacing to SPA	***parameter files (OEs, beamline), source files*** ***system calls of SPA-routine, result files***

User interfaces for PHASE

The old PHASE graphical user interface (GUI) was based on Motif widgets and graphic routines of the CERNLIB. Recently, the interface of the PHASE package has been upgraded: The Stationary Phase Approximation part is now based on the state-of-the-art qt and qtw widget set. Motif libraries and the CERNLIB are no longer required, which makes installations on standard Linux systems more straightforward. The Fourier Optics propagation routines, the related graphic output routines, and the data handling - including data compression to HDF5 format - are operated from IDL. Both PHASE packages for SPA and FO communicate via parameter files describing the optical elements and the beamline and standardized data formats for the electric fields.

5. ACKNOWLEDGMENT

The authors thank F. Siewert, Helmholtz-Zentrum Berlin, for providing the surface profile measurements and for discussions about state-of-the-art mirror fabrication accuracies. The authors thank also T. Zeschke, Helmholtz-Zentrum Berlin, for fruitful discussions on diaboloid mirrors.

REFERENCES

[1] Mandel L., Wolf, E., *Optical Coherence and Quantum Optics*, Cambridge University Press, Cambridge, England (1995).
[2] Bahrdt, J., "Fourth Order Optical Aberrations and Phase Space Transformation for Reflection and Diffraction Optics," Appl. Optics 34(1), 114-127 (1995).
[3] Bahrdt, J. "Wave Front Propagation: Design Code for Synchrotron Radiation Beam Lines," Appl. Optics 36(19), 4367-4381 (1997).
[4] Bahrdt, J. "Wavefront Tracking Within the Stationary Phase Approximation," Phys. Rev. Special Topics AB 10, 060701-1-15 (2007).
[5] Hearn, A. C., "REDUCE 3.5, A General Purpose Algebra System," RAND, Santa Monica, California (1993), http://www.uni-koeln.de/REDUCE/ .
[6] Siewert, F., Buchheim, J., Zeschke, T., "Characterization and calibration of 2nd generation slope measuring profiler," Nucl. Instrum. Methods A, 616, 119-127 (2010), doi: 101016/J.nima.2009.12.033.
[7] Siewert, F., Private communication, Helmholtz-Zentrum Berlin, Berlin, Germany.
[8] Zeschke, T., "Surface descriptions of diaboloid mirrors," Annual report, BESSY, Germany (2007).
[9] McKinney, W. R., Glossinger, J. M., Padmore, H. A., Howells, M. R., "Optical Path Function Calculation of an Incoming Cylindrical Wave," Proc. of SPIE, Vol. 7448-9, 1-8 (2009).

[10] Sawhney, K. J. S., Alcock, S. G., Signorato, R., "A Novel Adaptive Bimorph Focusing Mirror and Wavefront Corrector with Sub-Nanometer Dynamical Figure Control," Proc. of SPIE, Vol. 7803 (2010), doi: 10.1117/12.861593.
[11] Bahrdt, J., Flechsig, U., Senf, F., "Beamline Optimization and Phase Space Transformation," Rev. Sci. Instrum. 66, 2719-2723 (1995).
[12] Chubar, O., "Numerical Methods and Simulation Software for the Emission and Propagation of Fully- and Partially Coherent Synchrotron Radiation Wavefronts," SMEXOS workshop, ESRF, Grenoble, France, February 2009.